

# Lawrence Berkeley National Laboratory

## Lawrence Berkeley National Laboratory

### **Title**

Dopant-induced band filling and bandgap renormalization in CdO:In films

### **Permalink**

<https://escholarship.org/uc/item/91r5t09d>

### **Author**

Zhu, Yuankun

### **Publication Date**

2013-04-19

### **DOI**

10.1088/0022-3727/46/19/195102

Peer reviewed

Published in

J. Phys D: Appl. Phys. 46 (2013) 195102.

<http://dx.doi.org/10.1088/0022-3727/46/19/195102>

## **Dopant-induced band filling and bandgap renormalization in CdO:In films**

**Yuankun Zhu<sup>1</sup>, Rueben J. Mendelsberg<sup>2,3</sup>, Jiaqi Zhu<sup>1</sup>, Jiecai Han<sup>1</sup> and André Anders<sup>2</sup>**

<sup>1</sup>Center for Composite Materials and Structures, Harbin Institute of Technology, Harbin 150080, China

<sup>2</sup>Plasma Applications Group, Lawrence Berkeley National Laboratory, Berkeley, California, 94720

<sup>3</sup>Materials Science Division, Argonne National Laboratory, Argonne, Illinois, 60439

Email: zhujq@hit.edu.cn (Jiaqi Zhu)

### **Acknowledgment**

Research was supported by the LDRD Program of Lawrence Berkeley National Laboratory, by the Assistant Secretary for Energy Efficiency and Renewable Energy, Office of Building Technology, of the U.S. Department of Energy under U.S. Department of Energy Contract No. DE-AC02-05CH11231. Additional support was provided by the National Natural Science Foundation of China (Grant No.51072039 and 51222205), and the Ph.D. Programs Foundation of the Ministry of Education of China (20112302110036).

### **DISCLAIMER**

This document was prepared as an account of work sponsored by the United States Government. While this document is believed to contain correct information, neither the United States Government nor any agency thereof, nor The Regents of the University of California, nor any of their employees, makes any warranty, express or implied, or assumes any legal responsibility for the accuracy, completeness, or usefulness of any information, apparatus, product, or process disclosed, or represents that its use would not infringe privately owned rights. Reference herein to any specific commercial product, process, or service by its trade name, trademark, manufacturer, or otherwise, does not necessarily constitute or imply its endorsement, recommendation, or favoring by the United States Government or any agency thereof, or The Regents of the University of California. The views and opinions of authors expressed herein do not necessarily state or reflect those of the United States Government or any agency thereof or The Regents of the University of California.

## Abstract

The effect of carrier concentration on the Fermi level and bandgap renormalization in over 30 indium-doped cadmium oxide (CdO:In) films with carrier concentrations ranging from 1 to  $15 \times 10^{20} \text{ cm}^{-3}$  was studied by using the two band **k·p** model with electron-electron and electron-ion interactions. It is shown that the Tauc relation, which is based on parabolic valence and conduction bands, overestimates the optical bandgap in CdO films. Theoretical calculations of the optical bandgap give good agreement with experiments by taking into account the Burstein-Moss effect for a nonparabolic conduction band and bandgap renormalization effects. The band filling and bandgap renormalization in these CdO:In films are about 0.5~1.2 eV and 0.1~0.3 eV, respectively.

**PACS numbers:** 73.61.Ga, 78.66.Hf, 72.80.Ey, 71.20.Mq

## Introduction

Transparent conductive oxides (TCOs) have attracted much interest due to their tremendous importance in applications such as displays, photovoltaic cells, optical communications, gas sensors, and thin-film resistors [1-3]. Cadmium oxide (CdO) exhibiting high electrical conductivity and optical transparency is a promising TCO material. Due to their outstanding properties, undoped CdO films or those doped with trivalent elements have been fabricated by various techniques [4-8]. However, there is still controversy regarding the optical bandgap of CdO [6]. Table 1 shows a large dispersion of the optical bandgap as a function of carrier concentration as taken from recent literature. All the reported optical bandgaps in table 1 were obtained from Tauc plots [9] of  $\alpha^2$  [or  $(ahv)^2$ ] versus  $hv$  as derived from transmittance measurements (with some groups also accounting for reflectance). Under most circumstances, it has been ignored that the Tauc relation is based on parabolic valence and conduction bands. As such, the Tauc relation is extensively misused to determine the optical bandgap in doped CdO since the conduction band exhibits clear nonparabolicity [4, 5, 10]. Thus, optical bandgaps obtained from Tauc plots may add controversy when studying the bandgap shift. This is especially true if the object is to determine the carrier-concentration-dependent effective mass due to the conduction-band nonparabolicity.

For heavily doped TCOs, the bandgap shift is the result of two competing effects: bandgap widening via the Burstein-Moss effect, and renormalization due to many-body interactions [11, 12]. In this study, the optical bandgap of many indium-doped cadmium oxide (CdO:In) thin films were investigated using the two band **k·p** model [13] which proved successful for InN [14],  $\text{Ga}_x\text{In}_{1-x}\text{N}$  [15], ZnO [16], and CdS [16]. Though Kane's two band **k·p** model was derived from InSb which shows a different valence band dispersion shape at the Gamma point compared to CdO, this model has been previously used to predict the Fermi level in CdO films and good agreement with the experimental data was obtained [5, 17]. Despite the upward valence band at the Gamma point [18], the two band **k·p** model is generally valid for predicting the bandgap shift in CdO. In any case, renormalization due to electron-electron and electron-ion interactions must be accounted for to accurately describe the measured data.

## 1. Experiment

Pulsed filtered cathodic arc deposition (PFCAD) was utilized to grow the CdO:In films. Separate cadmium and indium rods were used as two source cathodes and were alternately pulsed in order to control the doping level between 0 and 9%. Borosilicate glass microscope slides and c-axis sapphire were used as the substrates. The CdO:In films were grown in oxygen pressures of 3~7 mTorr and at substrate temperatures ranging from room temperature to 425 °C. Optimized electrical properties were typically achieved in 7 mTorr oxygen with a substrate temperature of about 230 °C. Material of similar quality was deposited on the glass and sapphire substrates. Most of the samples were about 230 nm thick. Some thicker films of around 460 nm were also deposited. Details of the growth process have been described elsewhere [8].

Extensive descriptions of the properties of these arc-grown CdO films can be found in our previous work [8], and they are summarized here. X-ray diffraction showed that the as-deposited CdO:In films are polycrystalline with some preferred orientation along the (200) direction. The transmittance of glass substrate with about 230 nm thick CdO:In films is over 80% in the 500~1300 nm wavelength range as measured by a Perkin Elmer Lambda 950 dual beam photo-spectrometer. The carrier concentration was measured in the Van der Pauw geometry using an Ecopia HMS-3000 system with a 0.6 T magnetic field. It ranges from about  $1 \times 10^{20} \text{ cm}^{-3}$  in the undoped films to as high as  $1.5 \times 10^{21} \text{ cm}^{-3}$  in the heavily doped CdO films. These high quality arc-grown CdO and CdO:In films show a Hall mobility of 70~150  $\text{cm}^2/\text{Vs}$ .

## 2. Results and discussions

### 3.1 Theoretical bandgap calculation

CdO with high carrier concentration shows a nonparabolic conduction band. This nonparabolicity results from the  $\mathbf{k} \cdot \mathbf{p}$  interaction across the direct gap between the conduction and valence bands in heavily doped semiconductors [13, 14]. Neglecting perturbations from remote bands, an analytical form of the conduction band dispersion obtained by solving Kane's two band  $\mathbf{k} \cdot \mathbf{p}$  model is given by [13, 14]:

$$E_c(k) = E_G + \frac{\hbar^2 k^2}{2m_0} + \frac{1}{2} \left( \sqrt{E_G^2 + 4E_P \frac{\hbar^2 k^2}{2m_0}} - E_G \right) \quad (1)$$

where  $E_G$  is the direct bandgap energy of undoped CdO,  $k$  is the wave vector,  $m_0$  is the (bare) electron mass, and  $E_P$  is an energy parameter related to the momentum matrix element. Due to the nonparabolicity of the conduction band, the effective electron mass is  $k$ -dependent [19]:

$$m^*(k) = \frac{\hbar^2 k}{dE_c(k)/dk} \quad (2)$$

At the Fermi level, the effective mass is evaluated from the Fermi wave vector  $k_F = (3\pi^2 n)^{1/3}$ . Using  $E_G = 2.16 \text{ eV}$  [4], the effective mass calculated as a function of electron concentration for different  $E_P$  values is shown in figure 1. For the measured data shown in figure 1, the electron effective mass ( $m^*$ ) of each CdO:In film was calculated from the

(angular) Drude plasma frequency ( $\omega_p$ ) using:

$$m^* = \frac{ne^2}{\epsilon_0 \omega_p^2} \quad (3)$$

where  $n$  is the electron concentration,  $e$  is the elementary charge, and  $\epsilon_0$  is the permittivity of free space. For these CdO and CdO:In samples,  $\omega_p$  was obtained by simultaneously fitting the NIR transmittance and reflectance of each film, and  $n$  was taken from Hall measurements [10]. Using Pisarkiewicz's model [20], it has been observed that the nonparabolicity factor and the band edge effective mass of arc-grown CdO:In films are about  $0.5 \pm 0.2 \text{ eV}^{-1}$  and  $0.16 \pm 0.05 m_0$ , respectively [10]. The obtained values are in line with the results using the alpha approximation which was derived from Kane's two band  $\mathbf{k}\cdot\mathbf{p}$  model [21].

Figure 1 shows that  $m^*$  calculated from the  $\mathbf{k}\cdot\mathbf{p}$  conduction band dispersion is strongly dependent on  $n$ . Using  $E_p=6.5 \text{ eV}$  gives reasonably good agreement with the measured  $m^*$  values from the NIR data when taking into account the measurement uncertainties. This result is a bit lower than  $E_p=7.5 \text{ eV}$  obtained by Segura *et al.* [6] but it is still in agreement within the error range. However, in their calculation,  $E_p$ ,  $m^*$ , and  $E_G$  were simultaneously fit from the optical bandgap and they did not account for bandgap renormalization. For comparison, ZnO has  $E_p=13.4 \text{ eV}$  and CdS shows about  $14 \text{ eV}$  [14, 16]. A large spread was found for GaN and InN. For GaN,  $E_p$  ranges from about  $7.7 \text{ eV}$  [22] to a maximum value of  $18.6 \text{ eV}$  [16], and InN shows  $E_p$  about  $9.5 \text{ eV} \sim 18 \text{ eV}$  [14, 23]. Taking  $E_p=6.5 \text{ eV}$  into equation (1), the conduction band dispersion energy of CdO can be obtained. To study the effect of  $E_p$  carefully, the upper and lower bounds for  $E_p$  fitting results showing about  $8.5 \text{ eV}$  and  $4.5 \text{ eV}$  are also used for conduction band dispersion calculation.

Besides the Burstein-Moss band filling, bandgap renormalization effects in CdO:In films must also be taken into account. Bandgap renormalization results from the electron-electron and electron-ionized impurity interactions. According to the random perturbation theory by Berggren and Sernelius (BS model) [11], the down-shift of the conduction band due to the electron-electron interaction is (SI units):

$$\Delta E_{e-e} = \frac{e^2 k_F}{2\pi^2 \epsilon_0 \epsilon_s} + \frac{e^2 \lambda}{8\pi \epsilon_0 \epsilon_s} \left[ 1 - \frac{4}{\pi} \tan^{-1} \left( \frac{k_F}{\lambda} \right) \right] \quad (4)$$

where  $\lambda = 2/\sqrt{\pi} (k_F/a_B)^{1/2}$  is the Thomas-Fermi screening wave vector,  $\epsilon_s=21.9$  is the static dielectric constant of CdO [24], and  $a_B = 4\pi \epsilon_0 \epsilon_s \hbar^2 / (m^* e^2)$  is the effective Bohr radius. The contribution of the electron-ionized impurity interactions to the conduction band edge shift is [11]:

$$\Delta E_{e-i} = \frac{e^2 n}{\epsilon_0 \epsilon_s a_B \lambda^3} \quad (5)$$

It should be mentioned that another useful expression called the Jain model could also be utilized to estimate the bandgap renormalization in CdO films [25]. In fact, the Jain model, which has been demonstrated to be valid for AZO, ITO and other IV, III-V, and II-VI semiconductors [26-28], has a similar physical meaning as the BS model but it is less rigorous

due to its simplified derivation. In this study, compared with the BS model, the Jain model gives a 0.04~0.06 eV larger result depending on the carrier concentration but exhibits a very similar trend.

Taking the conduction-band nonparabolicity and the many-body interaction effects into account, the theoretical bandgap for CdO films can be calculated as a function of carrier concentration.

### 3.2 Experimentally measured bandgap

Optical bandgaps of thin films can be evaluated from the absorption curves. Using the transmittance and reflectance, the absorption coefficient ( $\alpha$ ) is calculated by [29].

$$T(h\nu) = \frac{(1 - R)^2 \exp\{-\alpha(h\nu)d\}}{1 - R^2 \exp\{-2\alpha(h\nu)d\}} \quad (6)$$

where  $d$ ,  $T$ , and  $R$  are film thickness, transmittance, and reflectance, respectively. In figure 2, it is observed that the absorption edge blueshifts with increasing carrier concentration. Importantly, a lower energy absorption edge is calculated if the reflectance is neglected, as shown in figure 2, resulting in a measured optical bandgap which is reduced by 0.02~0.05 eV. In order to avoid using the parabolic Tauc relation in this inherently nonparabolic system, the bandgap of CdO:In films is calculated using the first derivative of the transmittance spectra from a pseudo-Voigt fit [30]. As shown in figure 3, the transmittance-derived bandgap is typically about 0.1~0.3 eV lower than that obtained from a Tauc analysis of the same spectra [8]. In any case, a clear Burstein-Moss shift of the optical bandgap is observed with increasing carrier concentration.

When comparing the theoretical bandgaps calculated by accounting for nonparabolicity and renormalization, good agreement with the transmittance-derived bandgaps is observed in figure 3. The upper and lower bounds of theoretically calculated bandgaps are also shown in figure 3. All the parameters used in the calculations of the bandgap ( $E_G$ ,  $E_P$ ,  $\epsilon_s$ ) have been determined from independent measurements and no parameter has been adjusted further to achieve the good agreement in figure 3. Thus, the data show that the Burstein-Moss shift and bandgap renormalization in these CdO:In films are about 0.5~1.2 eV and 0.1~0.3 eV, respectively. For comparison, the optical bandgaps taken from the literature and listed in table 1 are also shown in figure 3. Importantly, it can be seen that the Tauc relation overestimates the optical bandgap in these CdO:In films and the transmittance-derived values are in better agreement with theory. In contrast, Segura *et al.* reported an underestimation of the optical bandgap in CdO when using the Tauc relation [6]. Their underestimation was concluded by comparing the optical bandgaps of different CdO samples as a function of carrier concentration and not accounting for the non-negligible bandgap renormalization in CdO samples showing high carrier concentration. In this work, the overestimation of optical bandgap is directly deduced from separately obtained theoretical and experimental results using the same spectra from the same samples.

The Fermi level of the CdO:In films is calculated by using Kane's two band  $\mathbf{k}\cdot\mathbf{p}$  model and is shown in figure 4. The experimental data in the figure is obtained from the measured optical bandgap by removing the renormalization effects due to the electron-electron and electron-ion interactions. It can be seen that Kane's two band  $\mathbf{k}\cdot\mathbf{p}$  theory shows good

agreement with the experimental data. For comparison, the Fermi energy based on a parabolic conduction band is calculated by using the parabolic Burstein-Moss equation.

$$E_F = \frac{\hbar^2}{2m^*} (3\pi^2 n)^{2/3} \quad (7)$$

Using constant effective masses of  $0.17 m_0$  [10] and  $0.27 m_0$  [17], it is shown that the simple parabolic conduction band model calculating the bandgap shift overestimates the Fermi energy in CdO:In films with high carrier concentration.

### 3. Conclusions

We have shown the dopant-induced Burstein-Moss band filling and bandgap renormalization in undoped CdO and CdO:In films. By combining the nonparabolic dispersion of the conduction band and the bandgap renormalization effects, it is found that the Tauc relation overestimates the optical bandgap in CdO:In films. Bandgap widening in these films, as evaluated from the derivative of the measured transmittance spectra, can be well described by the **k.p** interaction model when the electron-electron and electron-ion interactions are properly accounted for. Compared with the **k.p** interaction model, the simple parabolic conduction band model overestimates the Burstein-Moss effect in the heavily doped CdO films.

### References

- [1] Ramirez A P 2007 Applied physics: oxide electronics emerge *Science* **315** 1377-8
- [2] Yan M, Lane M, Kannewurf C R and Chang R P H 2001 Highly conductive epitaxial CdO thin films prepared by pulsed laser deposition *Appl. Phys. Lett.* **78** 2342
- [3] Calnan S and Tiwari A N 2010 High mobility transparent conducting oxides for thin film solar cells *Thin Solid Films* **518** 1839-49
- [4] Jefferson P H, Hatfield S A, Veal T D, King P D C, McConville C F, Zúñiga-Pérez J and Muñoz-Sanjose V 2008 Bandgap and effective mass of epitaxial cadmium oxide *Appl. Phys. Lett.* **92** 022101
- [5] Speaks D T, Mayer M A, Yu K M, Mao S S, Haller E E and Walukiewicz W 2010 Fermi level stabilization energy in cadmium oxide *J. Appl. Phys.* **107** 113706
- [6] Segura A, Sánchez-Royo J F, García-Domene B and Almonacid G 2011 Current underestimation of the optical gap and Burstein-Moss shift in CdO thin films: A consequence of extended misuse of  $\alpha^2$ -versus-hv plots *Appl. Phys. Lett.* **99** 151907
- [7] Wang A 2001 Indium-cadmium-oxide films having exceptional electrical conductivity and optical transparency: Clues for optimizing transparent conductors *Proc. Nat. Acad. Sci.* **98** 7113-6
- [8] Zhu Y, Mendelsberg R J, Zhu J, Han J and Anders A 2012 Transparent and conductive indium doped cadmium oxide thin films prepared by pulsed filtered cathodic arc deposition *Appl. Surf. Sci.* **265** 738-44
- [9] Tauc J, Grigorovici R and Vancu A 1966 Optical properties and electronic structure of amorphous germanium *Physica Status Solidi* **15** 627-37

- [10] Mendelsberg R J, Zhu Y K and Anders A 2012 Determining the nonparabolicity factor of the CdO conduction band using indium doping and the Drude theory *J. Phys. D: Appl. Phys.* **45** 425302
- [11] Berggren K and Sernelius B 1981 Band-gap narrowing in heavily doped many-valley semiconductors *Phys. Rev. B* **24** 1971-86
- [12] Sernelius B E, Berggren K F, Jin Z C, Hamberg I and Granqvist C G 1988 Band-gap tailoring of ZnO by means of heavy Al doping *Phys. Rev. B* **37** 10244-8
- [13] Kane E O 1957 Band structure of indium antimonide *J. Phys. Chem. Solids* **1** 249-61
- [14] Wu J, Walukiewicz W, Shan W, Yu K, Ager J, Haller E, Lu H and Schaff W 2002 Effects of the narrow band gap on the properties of InN *Phys. Rev. B* **66** 201403
- [15] Donmez O, Gunes M, Erol A, Arikan M C and Balkan N 2011 High carrier concentration induced effects on the bowing parameter and the temperature dependence of the band gap of  $\text{Ga}_x\text{In}_{1-x}\text{N}$  *J. Appl. Phys.* **110** 103506
- [16] Shokhovets S, Ambacher O, Meyer B and Gobsch G 2008 Anisotropy of the momentum matrix element, dichroism, and conduction-band dispersion relation of wurtzite semiconductors *Phys. Rev. B* **78** 035207
- [17] Vasheghani Farahani S K, Muñoz-Sanjosé V, Zúñiga-Pérez J, McConville C F and Veal T D 2013 Temperature dependence of the direct bandgap and transport properties of CdO *Appl. Phys. Lett.* **102** 022102
- [18] Burbano M, Scanlon D O and Watson G W 2011 Sources of conductivity and doping limits in CdO from hybrid density functional theory *J. Am. Chem. Soc.* **133** 15065-72
- [19] Skierbiszewski C, Perlin P, Wisniewski P, Knap W, Suski T, Walukiewicz W, Shan W, Yu K M, Ager J W, Haller E E, Geisz J F and Olson J M 2000 Large, nitrogen-induced increase of the electron effective mass in  $\text{In}_y\text{Ga}_{1-y}\text{N}_x\text{As}_{1-x}$  *Appl. Phys. Lett.* **76** 2409-11
- [20] Pisarkiewicz T, Zakrewska K and Leja E 1989 Scattering of charge carriers in transparent and conducting thin oxide films with a non-parabolic conduction band *Thin Solid Films* **174** 217-23
- [21] Ridley B K 1999 *Quantum process in semiconductors* (New York: Oxford university press)
- [22] Im J S, Moritz A, Steuber F, Härle V, Scholz F and Hangleiter A 1997 Radiative carrier lifetime, momentum matrix element, and hole effective mass in GaN *Appl. Phys. Lett.* **70** 631-3
- [23] Pérez-Caro M, Rodríguez A G, Vidal M A and Navarro-Contreras H 2010 Infrared study of the absorption edge of  $\beta$ -InN films grown on GaN/MgO structures *J. Appl. Phys.* **108** 013507
- [24] Finkenrath H and Von Ortenberg M 1967 *Z. Angew. Phys.* **23** 323-8
- [25] Zhu Y, Mendelsberg R J, Zhu J, Han J and Anders A 2013 Structural, optical, and electrical properties of indium doped cadmium oxide films prepared by pulsed filtered cathodic arc deposition *J. Mater. Sci.* **48** 3789-97
- [26] Lu J G, Fujita S, Kawaharamura T, Nishinaka H, Kamada Y, Ohshima T, Ye Z Z, Zeng Y J, Zhang Y Z, Zhu L P, He H P and Zhao B H 2007 Carrier concentration dependence of band gap shift in n-type ZnO:Al films *J. Appl. Phys.* **101** 083705
- [27] Jain S C and Roulston D J 1991 A simple expression for band gap narrowing (BGN)



- in heavily doped Si, Ge, GaAs and  $\text{Ge}_x\text{Si}_{1-x}$  strained layers *Solid-State Electron.* **34** 453-65
- [28] Jain S C, McGregor J M and Roulston D J 1990 Band-gap narrowing in novel III-V semiconductors *J. Appl. Phys.* **68** 3747-9
- [29] Ghezzi C, Magnanini R, Parisini A, Rotelli B, Tarricone L, Bosacchi A and Franchi S 1995 Optical absorption near the fundamental absorption edge in GaSb *Phys. Rev. B* **52** 1463-6
- [30] Ferreira da Silva A, Veissid N, An C Y, Pepe I, Barros de Oliveira N and Batista da Silva A V 1996 Optical determination of the direct bandgap energy of lead iodide crystals *Appl. Phys. Lett.* **69** 1930-2
- [31] Li X, Young D L, Moutinho H, Yan Y, Narayanswamy C, Gessert T A and Coutts T J 2001 Properties of CdO thin films produced by chemical vapor deposition *Electrochem. Solid-State Lett.* **4** C43-C6
- [32] Ueda N, Maeda H, Hosono H and Kawazoe H 1998 Band-gap widening of CdO thin films *J. Appl. Phys.* **84** 6174-7
- [33] Dakhel A A 2011 Structural, optical and electrical measurements on boron-doped CdO thin films *J. Mater. Sci.* **46** 6925-31
- [34] Zheng B J, Lian J S, Zhao L and Jiang Q 2010 Optical and electrical properties of In-doped CdO thin films fabricated by pulse laser deposition *Appl. Surf. Sci.* **256** 2910-4
- [35] Ou F, Buchholz D B, Yi F, Liu B, Hseih C, Chang R P H and Ho S-T 2011 Ohmic Contact of Cadmium Oxide, a Transparent Conducting Oxide, to n-type Indium Phosphide *ACS Appl. Mater. Interfaces.* **3** 1341-5
- [36] Saha B, Thapa R and Chattopadhyay K 2008 Bandgap widening in highly conducting CdO thin film by Ti incorporation through radio frequency magnetron sputtering technique *Solid State Commun.* **145** 33-7
- [37] Lamb D and Irvine S J C 2009 Near infrared transparent conducting cadmium oxide deposited by MOCVD *Thin Solid Films* **518** 1222-4
- [38] Wang L, Yang Y, Jin S and Marks T J 2006 MgO(100) template layer for CdO thin film growth: Strategies to enhance microstructural crystallinity and charge carrier mobility *Appl. Phys. Lett.* **88** 162115
- [39] Metz A W, Ireland J R, Zheng J G, Lobo R, Yang Y, Ni J, Stern C L, Dravid V P, Bontemps N, Kannewurf C R, Poepelmeier K R and Marks T J 2004 Transparent conducting oxides: Texture and microstructure effects on charge carrier mobility in MOCVD-derived CdO thin films grown with a thermally stable, low-melting precursor *J. Am. Chem. Soc.* **126** 8477-92
- [40] Deokate R J, Salunkhe S V, Agawane G L, Pawar B S, Pawar S M, Rajpure K Y, Moholkar A V and Kim J H 2010 Structural, optical and electrical properties of chemically sprayed nanosized gallium doped CdO thin films *J. Alloys Compd.* **496** 357-63
- [41] Kumaravel R, Ramamurthi K and Krishnakumar V 2010 Effect of indium doping in CdO thin films prepared by spray pyrolysis technique *J. Phys. Chem. Solids* **71** 1545-9
- [42] Jin S, Yang Y, Medvedeva J E, Wang L, Li S, Cortes N, Ireland J R, Metz A W, Ni J,

Hersam M C, Freeman A J and Marks T J 2008 Tuning the properties of transparent oxide conductors dopant ion size and electronic structure effects on CdO-based transparent conducting oxides Ga- and In-doped CdO thin films grown by MOCVD *Chem Mater* **20** 220-30

Table 1 Recently reported optical bandgaps ( $E_g$ ) of CdO films with various carrier concentrations.

| Films  | $d$ (nm) | $n (\times 10^{20} \text{ cm}^{-3})$ | $E_g$ (eV) | Reference |
|--------|----------|--------------------------------------|------------|-----------|
| CdO    | 114      | 0.17                                 | 2.4        | [31]      |
| CdO    | 576      | 0.21                                 | 2.31       | [32]      |
| CdO    | 160      | 0.44                                 | 2.42       | [33]      |
| CdO    | 330      | 0.66                                 | 2.41       | [34]      |
| CdO    | 500      | 0.92                                 | 2.4        | [2]       |
| CdO    | 659      | 1.5                                  | 2.58       | [32]      |
| CdO    | 100      | 1.5                                  | 2.4        | [35]      |
| CdO    | 480      | 1.7                                  | 2.4        | [4]       |
| CdO    | 450      | 2.2                                  | 2.52       | [36]      |
| CdO    | 320      | 2.3                                  | 2.6        | [37]      |
| CdO    | 300      | 2.6                                  | 2.8        | [38]      |
| CdO    | 152      | 2.7                                  | 3.08       | [31]      |
| CdO    | 530      | 2.9                                  | 2.84       | [39]      |
| CdO    | 500      | 10.5                                 | 2.27       | [40]      |
| CdO    | 1630     | 12.4                                 | 3.05       | [39]      |
| CdO:In | 450      | 3.7                                  | 2.72       | [41]      |
| CdO:In | 200      | 9.3                                  | 3.18       | [42]      |
| CdO:In | 250      | 10.9                                 | 2.97       | [34]      |
| CdO:In | 150      | 15.1                                 | 3.1        | [7]       |

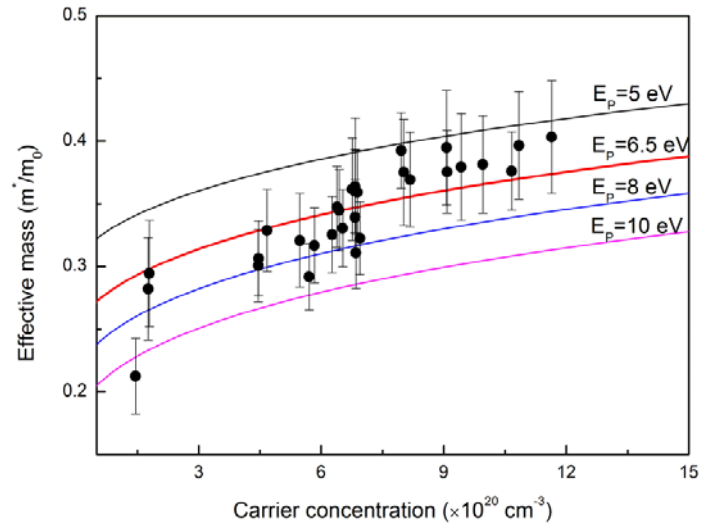


Figure 1 Effective mass of CdO:In films as a function of carrier concentration. The curves are calculated using equation (2) with different  $E_p$  values.

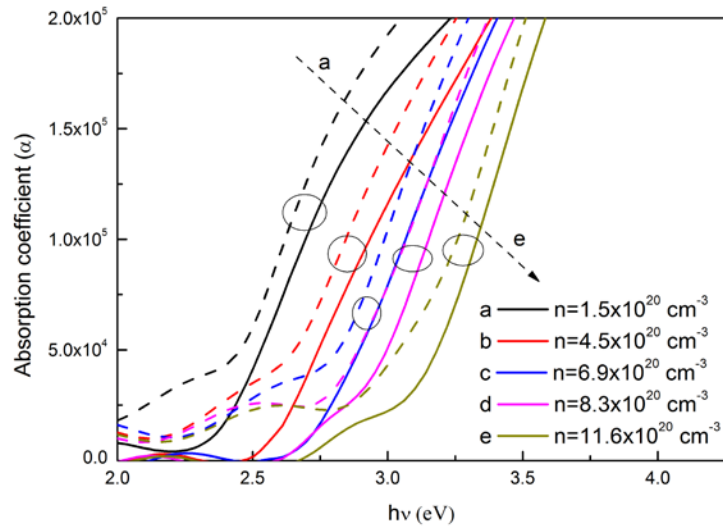


Figure 2 Absorption coefficient of CdO:In films with different carrier concentrations. The solid lines are calculated with the reflectance considered, and the dash lines are the same calculation but without including the reflectance.

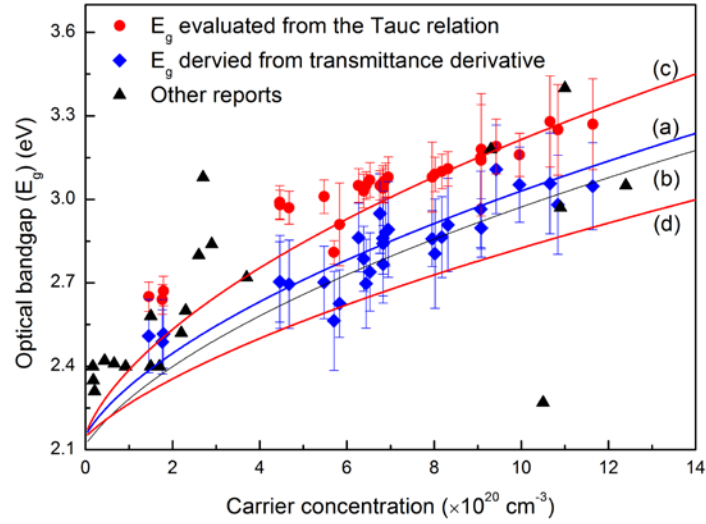


Figure 3 Optical bandgap of pure CdO and CdO:In films as a function of carrier concentration. The curves (a) and (b) are theoretically calculated bandgaps based on the BS model and the Jain model, respectively. The curves (c) and (d) are the upper and lower bounds of theoretically calculated bandgaps based on the BS model using  $E_p=8.5$  eV and 4.5 eV, respectively.

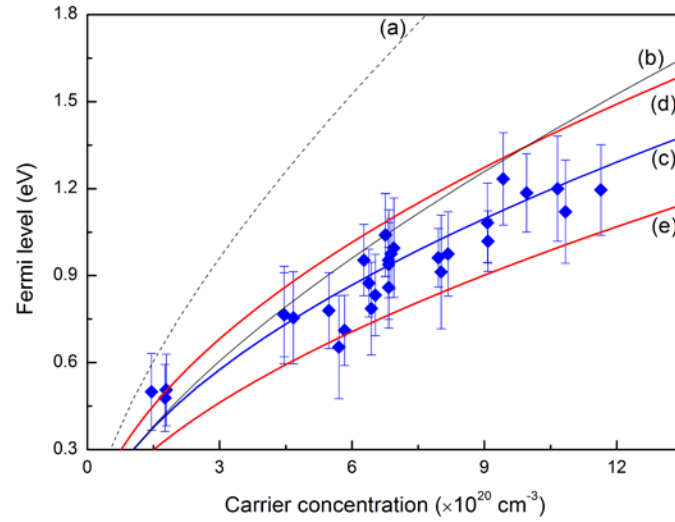


Figure 4 Fermi level of the CdO:In films with the conduction band edge taken as 0. The measured values come from optical bandgap measurements after bandgap renormalization has been accounted for. The fundamental bandgap of CdO is set to be 2.16 eV [4]. (a) and (b) a parabolic conduction band using a constant effective mass of  $0.17 m_0$  [10] and  $0.27 m_0$  [17], respectively, (c)  $\mathbf{k}\cdot\mathbf{p}$  model, (d) and (e) the upper and lower bonds of  $\mathbf{k}\cdot\mathbf{p}$  model using  $E_p=8.5$  eV and 4.5 eV, respectively.